physchem

MDPI

Article

Efficient Photocathode of an Ultrathin Organic p-n Bilayer Comprising p-Type Zinc Phthalocyanine and n-Type Fullerene for Hydrogen Peroxide Production

Yuika Sakaguchi, Kosuke Ikezoi and Toshiyuki Abe *

Department of Frontier Materials Chemistry, Graduate School of Science and Technology, Hirosaki University, 3 Bunkyo-cho, Hirosaki 036-8561, Japan
* Correspondence: tabe@hirosaki-u.ac.jp

Abstract

Hydrogen peroxide (H_2O_2) is a clean and environmentally friendly oxidant. At present, as an alternative to the conventional industrial procedure, namely, the anthraquinone method, a clean H_2O_2 production method is desired. The construction of an artificial photosynthetic system in which H_2O_2 can ideally be prepared from water and dioxygen (O_2) is a promising approach. In such a system, an organic p-n bilayer comprising zinc phthalocyanine (ZnPc, p-type) and fullerene (C_{60}, n-type) acts as a photocathode capable of O_2 reduction to H_2O_2, where loading gold (Au) onto the C_{60} surface is necessary to achieve the corresponding reaction. However, the enhancement of the photocathodic activity of the organic p-n bilayer for H_2O_2 formation remains a critical issue. In this study, the effect of the thickness of an organo-bilayer (organo-photocathode) on photocathodic activity for H_2O_2 production was investigated. When both ZnPc and C_{60} were thin (approximately 10 nm each in thickness), the photocathodic activity of the ZnPc/C_{60} organo-photocathode was approximately 3.4 times greater than that of the thick ZnPc/C_{60} bilayer (i.e., ZnPc = ca. 70 nm and C_{60} = ca. 120 nm). The thin ZnPc/C_{60} bilayer exhibited a built-in potential at the p-n interface, where efficient charge separation occurs, resulting in a high concentration of electrons available for O_2 reduction.

Keywords: hydrogen peroxide; oxygen reduction; photocathode; organic p-n bilayer

check for updates

Academic Editor: Aggelos Avramopoulos

Received: 8 October 2025
Revised: 27 October 2025
Accepted: 3 November 2025
Published: 5 November 2025

Citation: Sakaguchi, Y.; Ikezoi, K.; Abe, T. Efficient Photocathode of an Ultrathin Organic p-n Bilayer Comprising p-Type Zinc Phthalocyanine and n-Type Fullerene for Hydrogen Peroxide Production. *Physchem* **2025**, *5*, 49. https://doi.org/10.3390/physchem5040049

Copyright: © 2025 by the authors. Licensee MDPI, Basel, Switzerland. This article is an open access article distributed under the terms and conditions of the Creative Commons Attribution (CC BY) license (https://creativecommons.org/licenses/by/4.0/).

1. Introduction

Artificial photosynthesis reactions have been actively investigated to obtain fuels and chemicals such as molecular hydrogen [1–5], hydrogen peroxide (H_2O_2) [6–9], and some products from carbon dioxide (CO_2) [10–13]. H_2O_2 is a clean and environmentally friendly oxidizing agent, which is industrially produced using the anthraquinone method [14]. However, the industrial manufacturing method of H_2O_2 involves complex and multistep processes. In addition, significant energy consumption and organic waste emissions are major challenges limiting the commercialization of H_2O_2 [15]. Therefore, a clean and energy-saving H_2O_2 production method is urgently required to replace the conventional method.

H_2O_2 can be photocatalytically produced from water (H_2O) and oxygen (O_2) via the following redox reaction (Equation (1)):

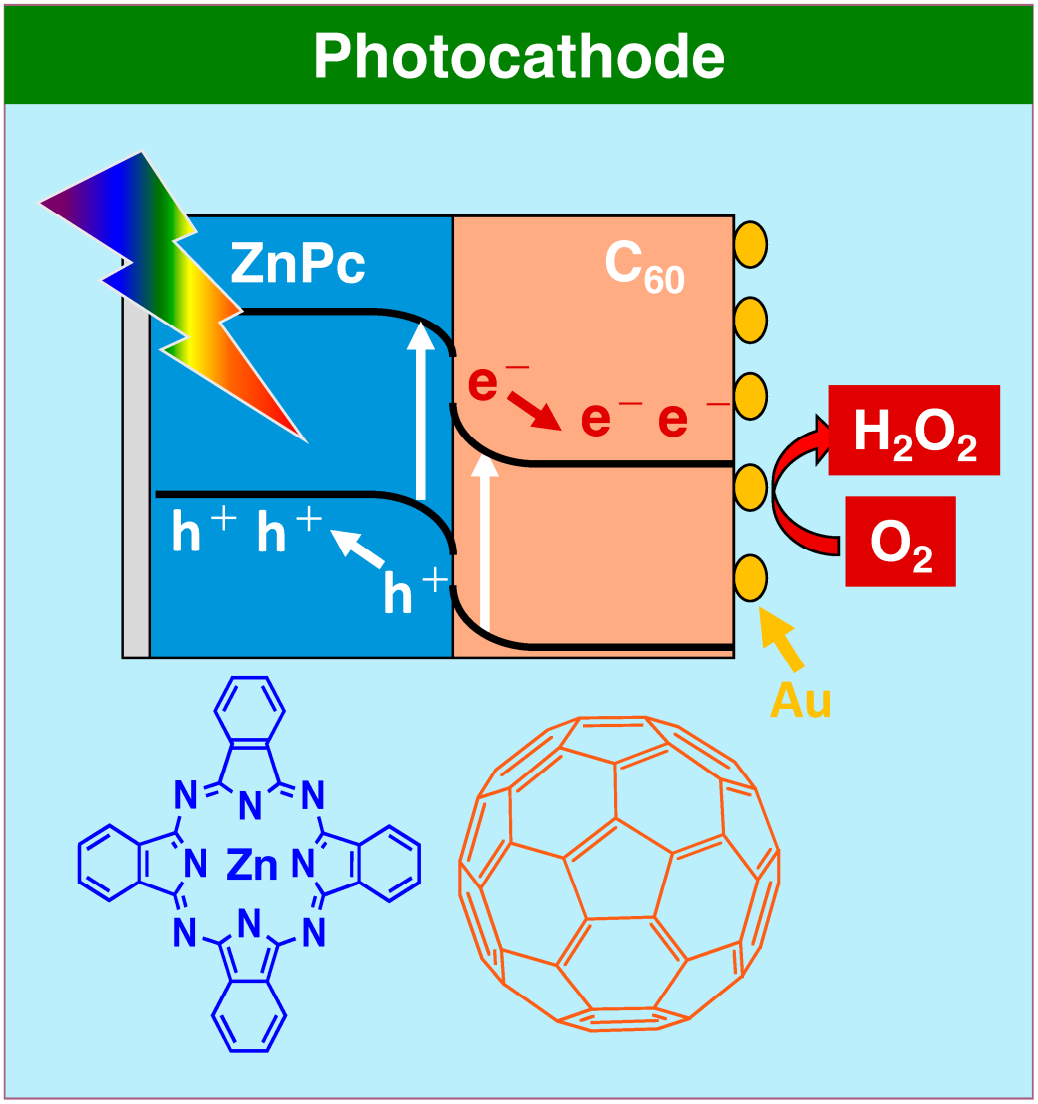
$$H_2O + 1/2\ O_2 \longrightarrow H_2O_2,\ \Delta G^\circ = +117\ kJ{\cdot}mol^{-1} \quad (1)$$

Such an uphill reaction, which corresponds to artificial photosynthesis, can be expected to proceed via photocatalysis. Many studies on photocatalytic H_2O_2 production have been conducted [6–9,16].

We have a track record of constructing an artificial photosynthesis system for water splitting featuring an organic p-n bilayer [17]. The water splitting system by Honda and Fujishima [18], comprising titanium dioxide (TiO_2) photoanode and Pt counter, is recognized to be a typical instance, but the overall splitting of water into O_2 and H_2 occurs only when a voltage bias is applied to the system. We reported the water splitting system composed of the TiO_2 photoanode and organo-photocathode, where bias-free water splitting was found to occur (see Scheme S1). In the system featuring a TiO_2 photoanode, our instance is an achievement that had not been discovered up to that time. In the Honda–Fujishima system, the oxidizing and reducing power generated at the TiO_2 photoanode is available to the water splitting into O_2 and H_2, while our system can utilize oxidizing and reducing power separately photogenerated at TiO_2 and organo-bilayer, respectively. In the latter, the electrons photogenerated at TiO_2 do not move to Pt counter for H_2 evolution (in the former), but to the holes remaining in the p-type layer of the organic p-n bilayer. Thus, it is summarized that, compared with the Honda–Fujishima system, the reason for bias-free water splitting in our system is kinetically favorable for the overall decomposition of water.

Based on this knowledge, we reported a photocatalytic system in which both a photocathode based on an organic p-n bilayer, comprising zinc phthalocyanine (ZnPc, p-type) and fullerene (C_{60}, n-type), and a photoanode based on co-catalyst-loaded bismuth vanadate ($BiVO_4$) were configured for H_2O_2 production (Scheme S1) [19]. In summary, the results of our previous study confirmed the production of H_2O_2 without the use of bias voltage in the photocatalytic system; however, the resulting efficiency was very low (i.e., <0.01% in maximum), and the rate-limiting step was the reduction of O_2 to H_2O_2 at the photocathode in which the gold (Au)-co-catalyst was loaded at the C_{60} surface of the organo-bilayer (denoted as ZnPc/C_{60}-Au). The activation of the ZnPc/C_{60}-Au photocathode is a critical issue to improve our previous system.

In the present study, the photoelectrochemical reduction of O_2 to H_2O_2 with ZnPc/C_{60}-Au was investigated in terms of the thickness of the organo-bilayer employed (Scheme 1). In our previous study on H_2O_2 production [19], the thickness of the ZnPc/C_{60} bilayer, which is recognized as optimal for reducing H^+ to H_2 [17,20,21], was used without any modification (i.e., ZnPc = ca. 70 nm and C_{60} = ca. 120 nm). In this study, the validity of this approach was examined, along with the novel optimization of the organo-bilayer used as the photocathode.



Scheme 1. Illustration of H_2O_2 formation occurring at ZnPc/C_{60}-Au photocathode.

2. Experimental

An indium tin oxide (ITO)-coated glass substrate (AGC Inc; sheet resistance: 8 $\Omega \cdot cm^{-2}$; transmittance: >85%; ITO thickness: 174 nm) was used as the electrode substrate. ZnPc (TCI) was purified via sublimation before use (sublimation conditions: temperature, 530 °C; pressure, ~2 × 10^{-2} Pa) [19,22]. Pure C_{60} (>99.5%, TCI) was used as received. The other reagents used in this study were of extra-pure grade.

The ZnPc/C_{60} organo-bilayer was fabricated on an ITO-coated glass substrate via vapor deposition (ULVAC KIKO Inc., Saito, Miyazaki, Japan, pressure: <1.0 × 10^{-3} Pa; deposition speed: ~0.03 $nm \cdot s^{-1}$) [17,21]. ZnPc was first coated on the ITO substrate, after which C_{60} was placed on top of the ZnPc layer. Au was photoelectrochemically deposited onto the C_{60} surface of the organo-bilayer under potentiostatic conditions, where a single-compartment cell was composed of an organo-bilayer-modified working electrode (effective area: 1 cm^2), a platinum counter electrode, and an Ag/AgCl (immersed in a saturated KCl solution; denoted as Ag/AgCl (sat.)) reference electrode in an acid solution (pH = 2) containing 5.0 × 10^{-4} $mol \cdot dm^{-3}$ $HAuCl_4 \cdot 4H_2O$ under an aerobic atmosphere. A potential of −0.2 V (vs. Ag/AgCl (sat.)) was applied to the modified ITO substrate for Au deposition. Photoelectrodeposition was performed using a potentiostat (HA-301, Hokuto Denko, Meguro-ku, Tokyo, Japan) equipped with a function generator (HB-104, Hokuto

Denko, Meguro-ku, Tokyo, Japan), a Coulomb meter (HF-201, Hokuto Denko, Meguro-ku, Tokyo, Japan), and an X–Y recorder under illumination. The amount of Au deposited was controlled by monitoring the amount of charge that passed during photoelectrodeposition (i.e., 0.04 C). The aforementioned electrochemical setup was used to measure voltammograms and photocurrents to obtain an action spectrum under potentiostatic conditions, but using a phosphoric acid solution (pH = 2) as the electrolyte. The light intensity was measured using a power meter (type 3A, Ophir Japan, Saitama, Japan). A halogen lamp was utilized for irradiating the photocathode with a typical intensity of approximately 100 $mW \cdot cm^{-2}$. For the irradiation in the action spectrum measurements, the light source was combined with a monochromator (S-10, Soma Optics, Hinode, Tokyo, Japan) to generate monochromatic light. The electrolysis experiment for reducing O_2 to H_2O_2 was conducted using a twin-compartment cell separated by a salt bridge (Scheme S2). The salt bridge preparation procedure is described elsewhere [17]. Calculation for the incident photon-to-current conversion efficiency (IPCE) and Faradaic efficiency (FE) are described in the Supplementary Materials (SM).

The crystal system of Au was analyzed by X-ray diffraction (XRD; SmartLab 9kW, Rigaku, Akishima, Tokyo, Japan). The surface of ZnPc/C_{60}−Au was observed via scanning electron microscopy (SEM; JSM-7000F, JEOL, Akishima, Tokyo, Japan). The absorption spectra of the organo-bilayer, single layers, and the peroxo–titanium complex solution (*vide infra*) were measured using a spectrophotometer (Lambda 35, PerkinElmer, Shelton, CT, USA).

The thickness of the organic p-n bilayer was determined by visible-light spectroscopy. The absorption spectra of both ZnPc [23] and C_{60} [24] obtained were identical to those previously reported, and their absorption coefficients indicated the thickness of the films used (Table S1). Since the additivity of the absorption coefficient should be preserved in the visible-light absorption spectrum of the bilayer, the two unknown parameters for each thickness were estimated by solving simultaneous equations for the absorbance at two different wavelengths (see SM for the simultaneous equations). Such estimation procedures for the thickness of organic p-n bilayers are described in the literature [22,25].

Quantification of H_2O_2 was performed using the so-called titanium sulfate method [26]: a 30% titanium(IV) sulfate solution (0.5 mL) was added to the electrolyte solution (2.5 mL) at the reduction site (see Scheme S2); when H_2O_2 was present in the solution, a peroxo–titanium complex was formed from a Ti^{4+} ion and an H_2O_2 molecule according to the following equation (Equation (2)):

$$Ti^{4+} + H_2O_2 + 2H_2O \rightarrow H_2TiO_4 + 4H^+ \quad (2)$$

By measuring the absorption spectrum of the resulting solution, the amount of H_2O_2 formed was determined from the absorbance of the peroxo–titanium complex at 410 nm (molar absorption coefficient: 674 $M^{-1} \cdot cm^{-1}$).

3. Results and Discussion

A typical X-ray diffraction pattern of Au particles is shown in Figure S1, in which Au is loaded on the C_{60} surface of the ZnPc/C_{60} organo-bilayer. The resulting pattern represents the formation of cubic Au, which is consistent with previous research [27]. The scanning electron microscopy image of the Au particles indicates the formation of fine Au particles in the order of <30 nm (Figure S2).

Voltammetric measurements were performed with regard to the thickness of the C_{60} and ZnPc layers. Figure 1a–c show the cyclic voltammograms (CVs) of the ZnPc/C_{60}-Au photocathode under an O_2 atmosphere, where the C_{60} layer thickness changed while the

ZnPc layer thickness remained constant (i.e., ZnPc = ca. 70 nm). In the dark, almost no electrochemical response was confirmed. However, when ZnPc/C_{60}-Au was irradiated, photocathodic currents were generated because of the reduction of O_2; in addition, the photocurrents increased with thinning of the C_{60} layer. Furthermore, the ZnPc thickness was varied while keeping the thickness of the thin C_{60} layer (i.e., C_{60} = 6~7 nm) constant. Similarly to the change with the C_{60} thickness, the thinner the ZnPc layer, the more enhanced the photocurrent (Figure 1d,e). These voltammetric results demonstrate efficient photocurrent generation at ZnPc/C_{60}-Au when thin ZnPc and C_{60} layers are used. By comparing the thinner layers (Figure 1e) with the thicker layers (Figure 1a), the photocurrent generated at −0.2 V (vs. Ag/AgCl (sat.)) was ca. 3~4 times higher with the former than with the latter. The photocathode shown in Figure 1e was subjected to repeated scans and demonstrated stable performance even after 10 scans (Figure 2).

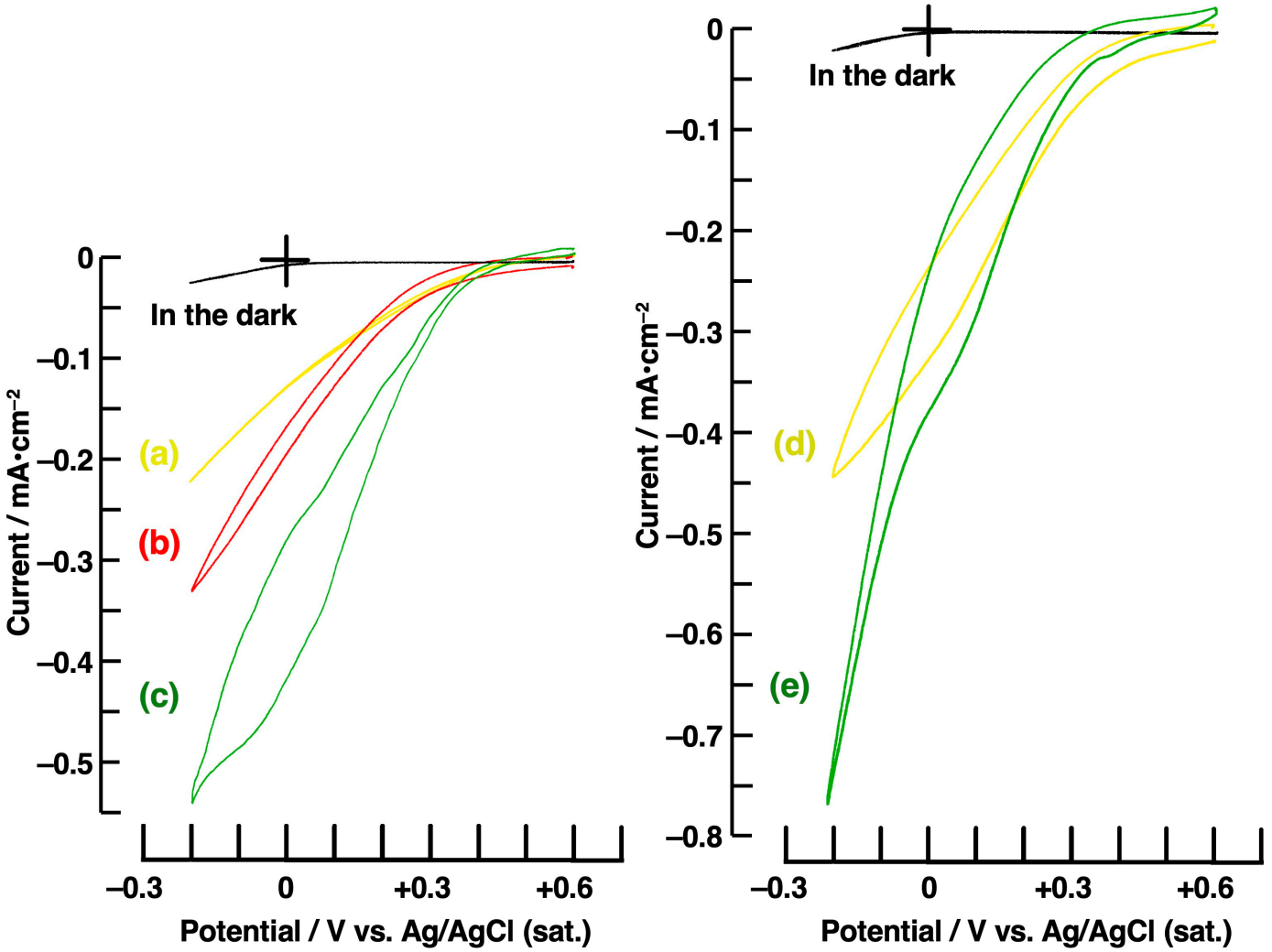


Figure 1. Cyclic voltammograms of ZnPc/C_{60}-Au under O_2 atmosphere. Electrolyte solution: aqueous H_3PO_4 solution (pH = 2); scan rate: 20 mV/s; C_{60} film thickness in (**a**–**c**) (with constant ZnPc thickness of ca. 70 nm): (**a**) 123 nm, (**b**) 46 nm, (**c**) 13 nm; ZnPc film thickness in (**d**,**e**) (with constant C_{60} thickness of ca. 6~7 nm): (**d**) 115 nm, (**e**) 11 nm; light intensity: 100 mW/cm^2; irradiation direction: from back of ITO-coated face.

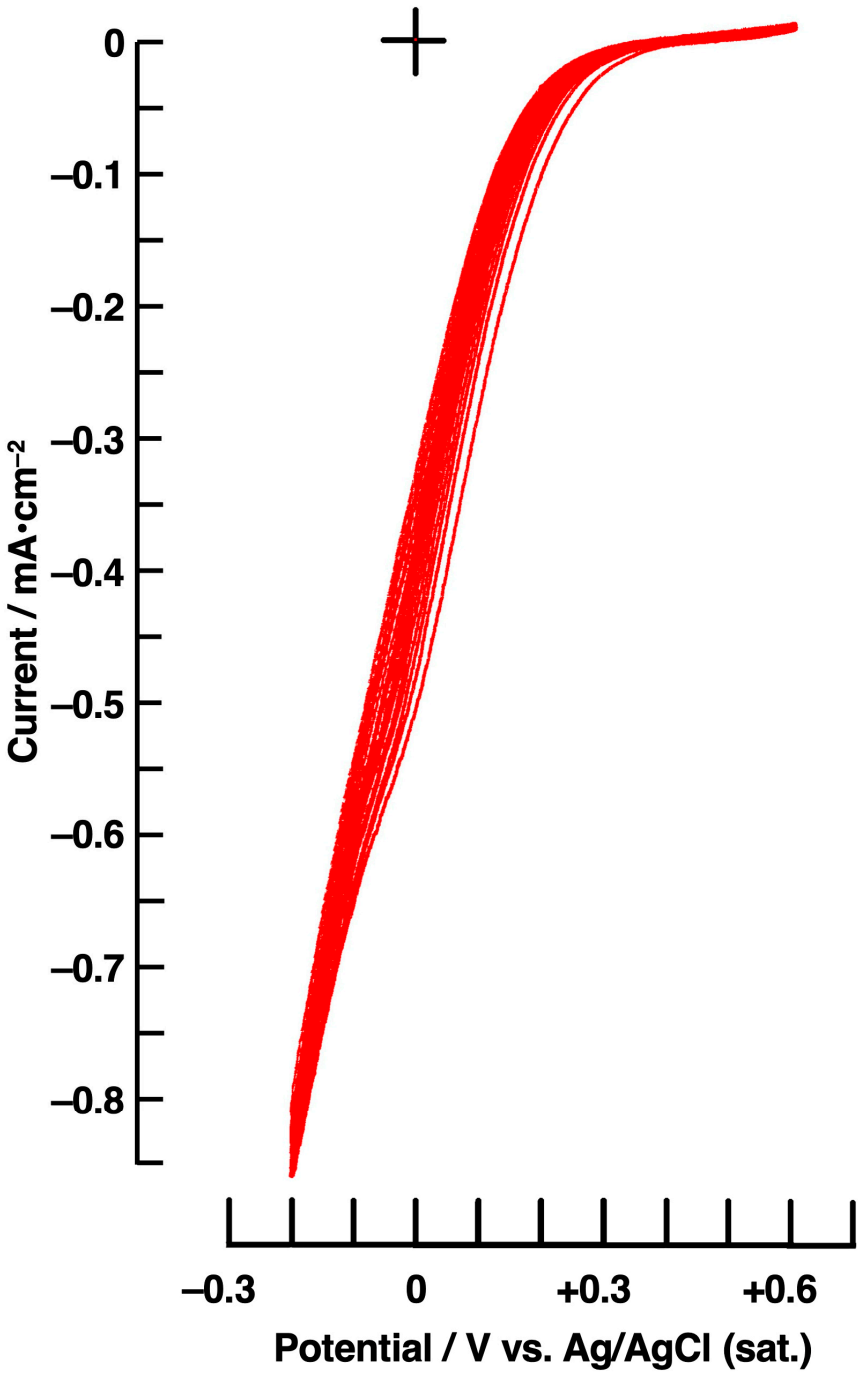


Figure 2. CVs of ZnPc/C_{60}-Au under O_2 atmosphere with repeated scans. Electrolyte solution: aqueous H_3PO_4 solution (pH = 2); scan rate: 20 mV/s; film thickness of ZnPc/C_{60} bilayer: 10 nm for ZnPc and 4 nm for C_{60}; light intensity: 100 mW/cm^2; irradiation direction: from the back of the ITO-coated face.

Using thin organo-bilayer that showed the most efficient characteristics, some types of ZnPc/C_{60}-Au were prepared by changing the amount of charge passed during Au deposition. Those CVs for the reduction of O_2 are shown in Figure 3. It can be considered that the amount of Au deposited corresponds to the charge amount (see SM). CV characteristics were improved with increasing the deposited amount of Au; however, when the Au amount was too large, the CV characteristics deteriorated. Thus, the conditions of Figures 1e and 2, where the thin organo-bilayers and constant amount of charge during Au deposition (i.e., 0.04 C) were employed, were confirmed to be optimum.

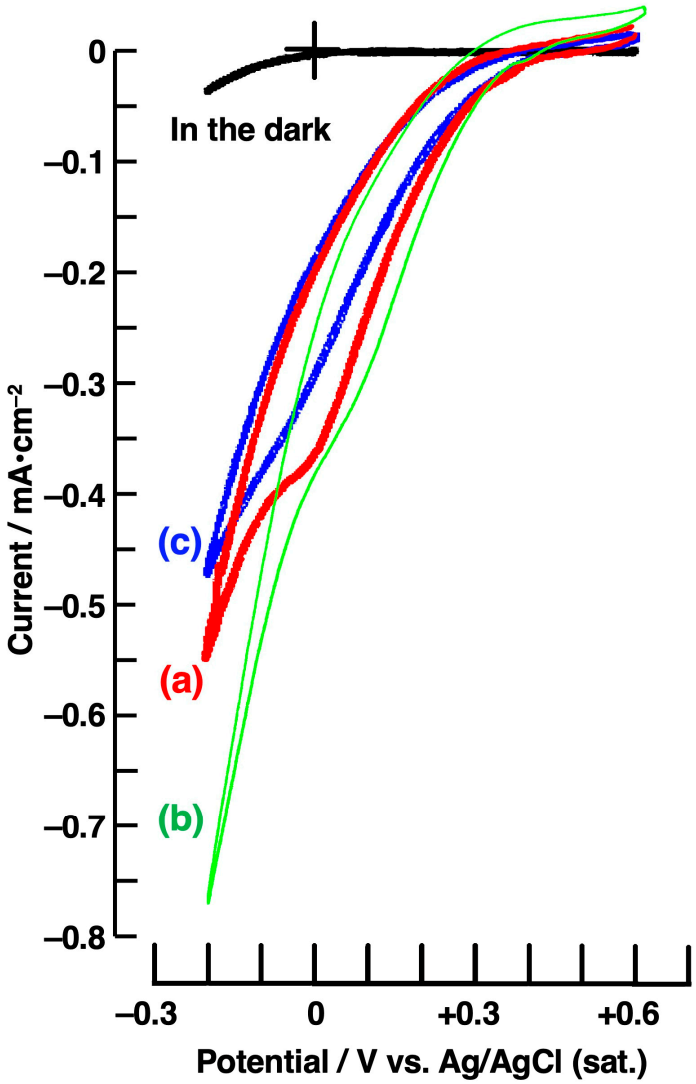


Figure 3. CVs of ZnPc/C_{60}-Au for O_2 reduction with changing the amount of charge passed during Au deposition ((**a**), 0.02 C; (**b**), 0.04 C; (**c**), 0.05 C). Electrolyte solution: aqueous H_3PO_4 solution (pH = 2); scan rate: 20 mV/s; film thickness of ZnPc/C_{60} bilayer: 11 nm for ZnPc and 6 nm for C_{60}; light intensity: 100 mW/cm^2; irradiation direction: from the back of the ITO-coated face.

To analyze the results of Figure 3, SEM images were observed with three types of Au loaded on the organo-bilayer (Figure S3). Comparing Figure S3a with Figure S3b, the particle size appears to increase with increasing charge amount. Figure S3c displays that the number of particles increase while maintaining the particle size with Figure S3b. In Figure 3, the surface concentration of electrons reaching the C_{60} surface should be constant because organo-bilayers of constant thickness were employed. As the number of Au particles increases, the number of active sites increases; however, the electron concentration per unit particle of Au decreases, and consequently, the activity of Au catalyst is diminished. Thus, it reveals that the deposition conditions of Figure S3b are optimum in the number and size of Au particles, efficiently highlighting the catalytic activity of Au.

Electrolysis for H_2O_2 production from O_2 was investigated with some types of organo-photocathodes. The typical data are summarized in Table 1. Supporting the voltammetric results, the amount of H_2O_2 produced increased with decreasing thickness of the organo-bilayer. The FE value for the formation of H_2O_2 was always >90% (see SM for the FE calculation), where the H_2O_2 amount in entry 3 was ca. 3.4 times larger than that in entry 1.

Table 1. Electrolysis data for H_2O_2 production by ZnPc/C_{60}-Au under illumination [a].

	ZnPc/nm	C_{60}/nm	Amount of H_2O_2/μmol
Entry 1	75	116	0.96
Entry 2	84	2.8	2.12
Entry 3	11	3.5	3.22

[a] Applied potential: −0.1 V vs. Ag/AgCl (sat.); electrolyte solution: aqueous H_3PO_4 solution (pH = 2); reaction time: 3 h; light intensity: 70 mW·cm^{-2}. Irradiation was performed from the back of the ITO-coated face. The deposition of Au onto the organo-bilayer was performed in the same way for each photocathode (see Experimental).

Action spectrum measurements were performed for the photocurrents generated at ZnPc/C_{60}-Au (Figure 4). Even when a thin ZnPc/C_{60} bilayer was used as photocathode, photocurrents were generated across the entire visible-light region. By comparing the resulting action spectrum with the single-layer ZnPc and C_{60} absorption spectra, the photocurrents originated from the absorption of both ZnPc and C_{60}: in other words, the photocurrent generation around at 460–490 nm, where the absorption of ZnPc is almost absent, can be induced by the sole absorption of C_{60}; photocurrents generated at wavelengths of >530 nm may have originated from ZnPc absorption.

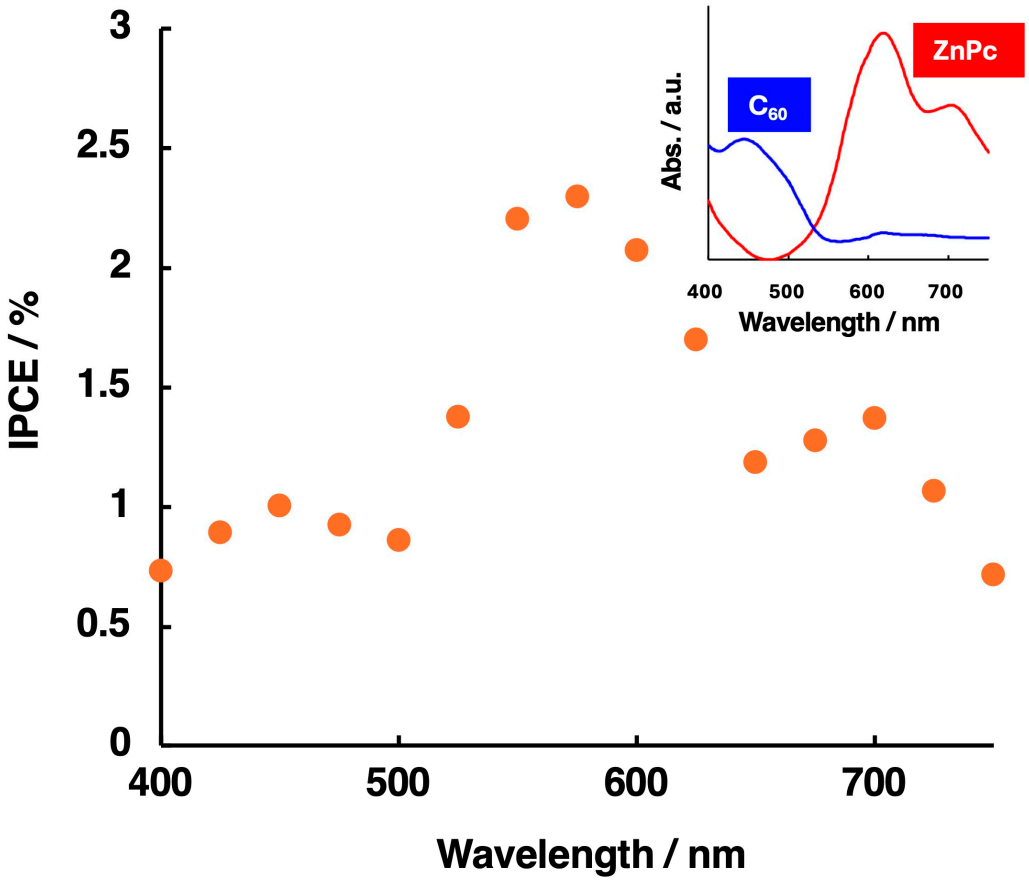


Figure 4. Action spectrum of ZnPc/C_{60}-Au photocurrents obtained under O_2 atmosphere. The inset shows the typical absorption spectra of single-layer ZnPc and C_{60}. Film thickness of ZnPc/C_{60} bilayer: 12 nm for ZnPc and 3 nm for C_{60}; applied potential: −0.1 V vs. Ag/AgCl; light intensity: 0.1 mW/cm^2; electrolyte solution: aqueous H_3PO_4 solution (pH = 2).

To gain insight into the thinner ZnPc/C_{60} organo-bilayer, rest potential was measured using single layers of ZnPc and C_{60}. The results are presented in Table 2. By comparing the rest potential values of n-type C_{60} and p-type ZnPc, the latter exhibited a more positive potential than the former; furthermore, the magnitude of the potential difference between

the ZnPc and C_{60} layers was independent of their thicknesses (i.e., ca. 0.5 V). These results demonstrate that built-in potential can be formed at the p-n interface even with a thin organo-bilayer, supporting the finding that series of photophysical events occur similar to photovoltaic cells of organic p-n bilayers [28]. Therefore, the photoelectrochemical reduction of O_2 to H_2O_2 at ZnPc/C_{60}-Au can be explained as follows. First, visible-light absorption occurs in both the ZnPc and C_{60} layers, and consequently, excitons are formed within both bilayers. The excitons attain at the p-n interface through excitation energy transfer, followed by the charge separation of excitons into electrons and holes at the hetero-interface. The photogenerated electrons move to the Au-coated C_{60} surface, thus resulting in the generation of reducing power for O_2 reduction. The reducing power induced the reduction of H^+ to H_2, as previously reported by our group [29]. The potential of O_2/H_2O_2 (+0.38 V vs. Ag/AgCl, at pH = 2) is more positive than that of H^+/H_2 (−0.32 V vs., Ag/AgCl, at pH = 2); thus, the O_2 reduction occurring at the ZnPc/C_{60} bilayer is thermodynamically reasonable. The kinetics of O_2 reduction should be proportional to the surface concentration of O_2 and the number of electrons available for H_2O_2 formation on the Au co-catalyst. Considering that the O_2 concentration was saturated under these experimental conditions, the photocathodic activity of ZnPc/C_{60}-Au for producing H_2O_2 can be associated with the concentration of electrons on the Au co–catalyst. When employing the thin bilayer as a photocathode, the transport distance of electrons from the p-n interface to Au can be shortened, thus effectively enhancing the electron concentration at Au. This may also relate to the reduced carrier recombination between electrons and holes.

Table 2. Rest potential measured using single-layer ZnPc and C_{60} [a].

	ZnPc/nm	C_{60}/nm	Rest Potential/V vs. Ag/AgCl (sat.)
Entry 1	-	142	–0.01
Entry 2	-	9.6	–0.06
Entry 3	86	-	0.44
Entry 4	9.6	-	0.43

[a] Electrolyte solution: aqueous H_3PO_4 solution (pH = 2); light intensity: 100 mW·cm^{-2}. Single-layer ZnPc and C_{60} were prepared on the ITO substrate, similar to the ZnPc/C_{60} bilayer. This measurement was performed under an Ar atmosphere. Irradiation was performed from the back of the ITO−coated face.

4. Conclusions

This study investigated the effect of the thickness of a ZnPc/C_{60} bilayer for the development of efficient photocathodes capable of H_2O_2 formation from O_2. The results demonstrate that a thin ZnPc/C_{60} bilayer acts as a superior photocathode when Au loaded on the C_{60} surface is employed as a co-catalyst. The thin bilayer reduced O_2 to H_2O_2 by approximately 3.4 times more than the thick bilayer used in our previous study. This result can be attributed to the high concentration of electrons available for H_2O_2 formation on the Au co-catalyst, which is achieved through a series of efficient photophysical processes that occur within the thin bilayer.

Supplementary Materials: The following supporting information can be downloaded at https://www.mdpi.com/article/10.3390/physchem5040049/s1. Scheme S1: Illustration of an artificial photosynthetic system for H_2O_2 formation; Scheme S2: Illustration of the electrolysis system used in this study; Determination of film thickness; Table S1: Absorption coefficients of ZnPc and C_{60}; Calculation for the incident photon-to-current conversion efficiency (IPCE) and Faradaic efficiency (FE); Figure S1: XRD pattern of Au deposited on C_{60} surface of ZnPc/C_{60} organo-bilayer; Figure S2: SEM images of C_{60} surface of ZnPc/C_{60} organo-bilayer with (a) and without (b) Au loading. Figure S3: SEM images of Au particles by changing the amount of charge passed during Au deposition (the amount of charge during Au deposition: (a), 0.02 C; (b), 0.04 C; (c), 0.06 C).

Author Contributions: Conceptualization, T.A.; validation, T.A.; investigation, Y.S. and K.I.; resources, T.A.; writing—original draft, T.A.; supervision, T.A.; project administration, T.A. All authors have read and agreed to the published version of the manuscript.

Funding: This research was funded by JSPS KAKENHI Grant Number JP22K05183 (T.A.).

Institutional Review Board Statement: Not applicable.

Informed Consent Statement: Not applicable.

Data Availability Statement: All data are available in the main text or the Supplementary Materials.

Acknowledgments: T. Abe acknowledges financial support from JSPS.

Conflicts of Interest: The authors declare no conflicts of interest.

References

1. Qi, Y.; Zhang, B.; Zhang, G.; Zheng, Z.; Xie, T.; Chen, S.; Ma, G.; Li, C.; Domen, K.; Zhang, F. Efficient overall water splitting of a suspended photocatalyst boosted by metal-support interaction. *Joule* **2024**, *8*, 193–203. [CrossRef]
2. Lin, L.; Ma, Y.; Vequizo, J.J.M.; Nakabayashi, M.; Gu, C.; Tao, X.; Yoshida, H.; Pihosh, Y.; Nishina, Y.; Yamakata, A.; et al. Efficient and stable visible-light-driven Z-scheme overall water splitting using an oxysulfide H_2 evolution photocatalyst. *Nat. Commun.* **2024**, *15*, 397. [CrossRef]
3. Xin, X.; Li, Y.; Zhang, Y.; Wang, Y.; Chi, X.; Wei, Y.; Diao, C.; Su, J.; Wang, R.; Guo, P.; et al. Large electronegativity differences between adjacent atomic sites activate and stabilize $ZnIn_2S_4$ for efficient photocatalytic overall water splitting. *Nat. Commun.* **2024**, *15*, 337. [CrossRef]
4. Fu, H.; Zhang, Q.; Liu, Y.; Zheng, Z.; Cheng, H.; Huang, B.; Wang, P. Photocatalytic Overall Water Splitting with a Solar-to-Hydrogen Conversion Efficiency Exceeding 2% through Halide Perovskite. *Angew. Chem. Int. Ed.* **2024**, *63*, e202411016. [CrossRef]
5. Takata, T.; Liu, L.; Hisatomi, T.; Domen, K. Best Practices for Assessing Performance of Photocatalytic Water Splitting Systems. *Adv. Mater.* **2024**, *36*, 2406848. [CrossRef]
6. Kondo, Y.; Mizutani, S.; Kuwahara, Y.; Mori, K.; Sekino, T.; Yamashita, H. Perfluoroalkyl-functionalization of zirconium-based metal–organic framework nanosheets for photosynthesis of hydrogen peroxide from dioxygen and water. *J. Mater. Chem. A* **2025**, *13*, 3701–3710. [CrossRef]
7. Xu, X.; Sui, Y.; Chen, W.; Huang, W.; Li, X.; Li, Y.; Liu, D.; Gao, S.; Wu, W.; Pan, C.; et al. The photocatalytic H_2O_2 production by metal-free photocatalysts under visible-light irradiation. *Appl. Catal. B* **2024**, *341*, 123271. [CrossRef]
8. Liu, T.; Pan, Z.; Vequizo, J.J.M.; Kato, K.; Wu, B.; Yamakata, A.; Katayama, K.; Chen, B.; Chu, C.; Domen, K. Overall photosynthesis of H_2O_2 by an inorganic semiconductor. *Nat. Commun.* **2022**, *13*, 1034. [CrossRef] [PubMed]
9. Kofuji, Y.; Isobe, Y.; Shiraishi, Y.; Sakamoto, H.; Tanaka, S.; Ichikawa, S.; Hirai, T. Carbon Nitride–Aromatic Diimide–Graphene Nanohybrids: Metal-Free Photocatalysts for Solar-to-Hydrogen Peroxide Energy Conversion with 0.2% Efficiency. *J. Am. Chem. Soc.* **2016**, *138*, 10019–10025. [CrossRef] [PubMed]
10. Wang, W.; Zhang, W.; Deng, C.; Sheng, H.; Zhao, J. Accelerated Photocatalytic Carbon Dioxide Reduction and Water Oxidation under Spatial Synergy. *Angew. Chem. Int. Ed.* **2024**, *63*, e202317969. [CrossRef]
11. Wang, L.; Qiu, C.; Chen, R.; Chen, X.; Ding, J.; Zhang, J.; Wan, H.; Guan, G. Constructing the facet junction on solid solution $BiOBr_{1-x}Cl_x$ for efficient photocatalytic CO_2 reduction with H_2O. *J. Alloys Compd.* **2024**, *985*, 174022. [CrossRef]
12. Nakamoto, T.; Iguchi, S.; Naniwa, S.; Tanaka, T.; Teramura, K. Surface Modifications of Heterogeneous Photocatalysts for Photocatalytic Conversion of CO_2 by H_2O as the Electron Donor. *ChemCatChem* **2024**, *16*, e202400594. [CrossRef]
13. Cao, F.; Zhang, X.; Niu, X.; Lin, X.; Wu, T.; Zhong, S.; Lin, H.; Zhao, L.; Bai, S. Upgrading Single S-Scheme Heterojunction to Multi-S-Scheme Ones for Better Synergy of Photocatalytic CO_2 Reduction and H_2O Oxidation: The Third Component Location Matters. *ACS Catal.* **2024**, *14*, 12529–12540. [CrossRef]
14. Riedl, H.J.; Pfleiderer, G. Preparation from Organic Compounds by the Alkyl-Anthraquinone Process. U.S. Patent Application No. C01B15/023, US2158525A, 16 May 1939.
15. Ciriminna, R.; Albanese, L.; Meneguzzo, F.; Pagliaro, M. Hydrogen Peroxide: A Key Chemical for Today's Sustainable Development. *ChemSusChem* **2016**, *9*, 3374–3381. [CrossRef] [PubMed]
16. Chen, H.-Y.; Huang, J.-R.; Liu, J.-C.; Huang, N.-Y.; Chen, X.-M.; Liao, P.-Q. Integration of Plasmonic Ag(I) Clusters and Fe(II) Porphyrinates into Metal–Organic Frameworks for Efficient Photocatalytic CO_2 Reduction Coupling with Photosynthesis of Pure H_2O_2. *Angew. Chem. Int. Ed.* **2024**, *63*, e202412553. [CrossRef] [PubMed]
17. Abe, T.; Fukui, K.; Kawai, Y.; Nagai, K.; Kato, H. A water splitting system using organo-photocathode and titanium dioxide photoanode capable of bias-free H_2 and O_2 evolution. *Chem. Commun.* **2016**, *52*, 7735–7737. [CrossRef]
18. Fujishima, A.; Honda, K. Electrochemical Photolysis of Water at a Semiconductor Electrode. *Nature* **1972**, *238*, 37–38. [CrossRef]

19. Ikezoi, K.; Chisaka, M.; Abe, T. Photocatalytic and photoelectrochemical production of hydrogen peroxide under acidic conditions in organic p-n bilayer/bismuth vanadate system. *Int. J. Electrochem. Sci.* **2022**, *17*, 221143. [CrossRef]
20. Abe, T.; Chiba, J.; Ishidoya, M.; Nagai, K. Organophotocatalysis System of p/n Bilayers for Wide Visible Light-Induced Molecular Hydrogen Evolution. *RSC Adv.* **2012**, *2*, 7992–7996. [CrossRef]
21. Abe, T.; Hiyama, Y.; Fukui, K.; Sahashi, K.; Nagai, K. Efficient p-zinc phthalocyanine/n-fullerene organic bilayer electrode for molecular hydrogen evolution induced by the full visible-light energy. *Int. J. Hydrogen Energy* **2015**, *40*, 9165–9170. [CrossRef]
22. Abe, T.; Miyakushi, S.; Nagai, K.; Norimatsu, T. Study of the factors affecting the photoelectrode characteristics of a perylene/phthalocyanine bilayer working in the water phase. *Phys. Chem. Chem. Phys.* **2008**, *10*, 1562–1568. [CrossRef]
23. Morikawa, T.; Adachi, C.; Tsutsui, T.; Saito, S. Multilayer-Type Organic Solar Cells Using Phthalocyanines and Perylene Derivatives. *Nippon Kagaku Kaishi* **1990**, *1990*, 962–967. [CrossRef]
24. Capobianchi, A.; Tucci, M. Ruthenium phthalocyanine thin films for photovoltaic applications. *Thin Solid Films* **2004**, *451*, 33–36. [CrossRef]
25. Abe, T.; Nakamura, K.; Ichinohe, H.; Nagai, K. Evaluation of photoanodic output on carbon cluster/phthalocyanine films with respect to the types of n-type conductors employed. *J. Mater. Sci.* **2012**, *47*, 1071–1076. [CrossRef]
26. Eisenberg, G.M. Colorimetric Determination of Hydrogen Peroxide. *Ind. Eng. Chem. Anal. Ed.* **1943**, *15*, 327–328. [CrossRef]
27. Swason, H.E.; Tatge, E. Standard X-ray diffraction powder patterns. *Natl. Bur. Stand. Circ.* **1953**, *539*, 33.
28. Tanaka, S.; Hanada, T.; Ono, K.; Watanabe, K.; Yoshino, K.; Hiromitsu, I. Improvement of power conversion efficiency of phthalocyanine/C_{60} heterojunction solar cells by inserting a lithium phthalocyanine layer at the indium-tin oxide/phthalocyanine interface. *Appl. Phys. Lett.* **2010**, *97*, 253306. [CrossRef]
29. Abe, T.; Tobinai, S.; Taira, N.; Chiba, J.; Itoh, T.; Nagai, K. Molecular Hydrogen Evolution by Organic p/n Bilayer Film of Phthalocyanine/Fullerene in the Entire Visible-Light Energy Region. *J. Phys. Chem. C* **2011**, *115*, 7701–7705. [CrossRef]

Disclaimer/Publisher's Note: The statements, opinions and data contained in all publications are solely those of the individual author(s) and contributor(s) and not of MDPI and/or the editor(s). MDPI and/or the editor(s) disclaim responsibility for any injury to people or property resulting from any ideas, methods, instructions or products referred to in the content.